Eur. Phys. J. C (2009) 62: 265–269
DOI 10.1140/epjc/s10052-009-1037-8

THE EUROPEAN PHYSICAL JOURNAL C

Regular Article - Experimental Physics

Energy and system dependence of high-p_T triggered two-particle near-side correlations

Christine Nattrass[a]
for the STAR Collaboration
WNSL, Yale University, 272 Whitney Ave., New Haven, CT 06520, USA

Received: 30 September 2008 / Revised: 17 March 2009 / Published online: 5 May 2009

Abstract Previous studies have indicated that the near-side peak of high-p_T triggered correlations can be decomposed into two parts, the *Jet* and the *Ridge*. We present data on the yield per trigger of the *Jet* and the *Ridge* from $d+\mathrm{Au}$, $\mathrm{Cu}+\mathrm{Cu}$ and $\mathrm{Au}+\mathrm{Au}$ collisions at $\sqrt{s_{NN}}=62.4$ GeV and 200 GeV and compare data on the *Jet* to PYTHIA 8.1 simulations for $p+p$. PYTHIA describes the *Jet* component up to a scaling factor, meaning that PYTHIA can provide a better understanding of the *Ridge* by giving insight into the effects of the kinematic cuts. We present collision energy and system dependence of the *Ridge* yield, which should help distinguish models for the production mechanism of the *Ridge*.

PACS 25.75.-q · 21.65.Qr · 24.85.+p · 25.75.Bh

1 Introduction

Previous studies demonstrated that there are two structures in the near-side peak in high-p_T triggered correlations in $\mathrm{Au}+\mathrm{Au}$ collisions at $\sqrt{s_{NN}}=200$ GeV. The *Jet* similar to what is observed in $d+\mathrm{Au}$, narrow in both azimuth ($\Delta\phi$) and pseudorapidity ($\Delta\eta$), and is similar to that expected from vacuum fragmentation. In contrast, the *Ridge* is narrow in azimuth but broad in pseudorapidity and has properties similar to the bulk [1, 2]. These studies test whether these conclusions hold for other collision systems and energies by comparing data from $\mathrm{Au}+\mathrm{Au}$ and $\mathrm{Cu}+\mathrm{Cu}$ collisions at $\sqrt{s_{NN}}=62.4$ GeV and $\sqrt{s_{NN}}=200$ GeV.

Several mechanisms have been proposed for the production of the *Ridge* [3–7] but there have been few calculations which can be directly compared to data. This is in part because there are many factors which must be considered when calculating the experimentally measured quantities. Because trends expected with changing collision energy and in nuclei collided should be easier to calculate theoretically, the results presented here should provide a good test of models for the production of the *Jet* and *Ridge*.

2 Method

Data from the STAR detector from year 3 $d+\mathrm{Au}$ collisions as $\sqrt{s_{NN}}=200$ GeV, year 4 $\mathrm{Au}+\mathrm{Au}$ collisions at $\sqrt{s_{NN}}=62.4$ GeV and $\sqrt{s_{NN}}=200$ GeV, and year 5 $\mathrm{Cu}+\mathrm{Cu}$ collisions at $\sqrt{s_{NN}}=62.4$ GeV and $\sqrt{s_{NN}}=200$ GeV were used for the comparison of collision systems and energies. Details of the STAR detector can be found in [8]. The primary detector used for these analyses was the STAR Time Projection Chamber (TPC.)

A high transverse momentum (p_T) particle is selected and the distribution of other particles in the event relative to that trigger particle in azimuth ($\Delta\phi$) and pseudorapidity ($\Delta\eta$) $\frac{d^2N}{d\Delta\phi d\Delta\eta}$ was determined. The p_T of the trigger and associated particles was restricted in order to reduce the soft background; unless otherwise mentioned $1.5\ \mathrm{GeV/c} < p_T^{associated} < p_T^{trigger}$ and $3.0 < p_T^{trigger} < 6.0$ GeV/c. $\frac{d^2N}{d\Delta\phi d\Delta\eta}$ is normalized by the number of trigger particles. This was corrected for the single particle efficiency and for detector acceptance, which is dependent on the collision system and energy, p_T, $\Delta\eta$, $\Delta\phi$, and collision multiplicity. Except for studies of N_{part} dependence, the $\mathrm{Cu}+\mathrm{Cu}$ data at both energies are for 0–60% centrality, $\mathrm{Au}+\mathrm{Au}$ data at $\sqrt{s_{NN}}=62.4$ GeV are for 0–80% centrality, and $\mathrm{Au}+\mathrm{Au}$ data at $\sqrt{s_{NN}}=200$ GeV are for 0–10% centrality. $d+\mathrm{Au}$ data are minimum bias.

The yield measured is the number of particles associated with the trigger particle within the limits on $p_T^{associated}$ and $p_T^{trigger}$. The *Ridge* was previously observed to be roughly

[a] e-mail: nattrass@rhig.physics.yale.edu

independent of $\Delta\eta$ within the acceptance of the STAR TPC [2]. To extract the yield it is assumed that the *Ridge* is independent of $\Delta\eta$. Previous studies have demonstrated that the *Jet* component extends to $|\Delta\eta| = 0.75$ in the p_T range studied here and that limited detector acceptance limits studies to $|\Delta\eta| < 1.75$ [1, 2, 9]. To determine the *Jet* yield Y_{Jet}, the projection of the distribution of particles $\frac{d^2N}{d\Delta\phi d\Delta\eta}$ is taken in two different ranges in pseudorapidity:

$$\frac{dY_{Ridge}}{d\Delta\phi} = 1/N_{trigger}\int_{-1.75}^{-0.75}\frac{d^2N}{d\Delta\phi d\Delta\eta}d\Delta\eta + 1/N_{trigger}\int_{0.75}^{1.75}\frac{d^2N}{d\Delta\phi d\Delta\eta}d\Delta\eta$$

$$\frac{dY_{Jet+Ridge}}{d\Delta\phi} = 1/N_{trigger}\int_{-0.75}^{0.75}\frac{d^2N}{d\Delta\phi d\Delta\eta}d\Delta\eta$$

where the former contains only the *Ridge* and the latter contains both the *Jet* and the *Ridge*. The jet-like yield on the near-side is the integral over $-1 < \Delta\phi < 1$:

$$Y_{Jet} = \int_{-1}^{1}\left(\frac{dY_{Jet+Ridge}}{d\Delta\phi} - \frac{0.75}{1}\frac{dY_{Ridge}}{d\Delta\phi}\right)d\Delta\phi.$$

The factor in front of the second term is the ratio of the $\Delta\eta$ width in the region containing the *Jet* and the *Ridge* to the width of the region containing only the *Ridge*. With this method for subtracting the *Ridge* contribution to Y_{Jet}, the systematic errors due to v_2 cancel out assuming that v_2 is roughly independent of $\Delta\eta$, a reasonable assumption in the mid-rapidity range $|\eta| < 1$ based on the available data [11, 12]. It is also assumed that the *Ridge* is independent of $\Delta\eta$.

To determine Y_{Ridge} the integration is done over the entire $\Delta\eta$ region to minimize the effects of statistical fluctuations in the determination of the background:

$$Y_{Ridge} = 1/N_{trigger}\int_{-1.75}^{1.75}\int_{-1}^{1}\frac{d^2N}{d\Delta\phi d\Delta\eta}d\Delta\phi d\Delta\eta - Y_{Jet}.$$

The integration over $\Delta\eta$ is done by bin counting. The integration over $\Delta\phi$ is done by fitting a Gaussian to the near-side. This partially compensates for a detector effect which causes lost tracks at $\Delta\phi \approx 0$ and $\Delta\eta \approx 0$; this effect is less than 10% in the p_T range studied here [10].

The combinatorial background is correlated in azimuth due to particles correlated indirectly with each other in azimuth due to their correlation with the reaction plane. This random background is given by

$$\frac{dY_{bkgd}}{d\phi} = B(1 + 2\langle v_2^{trigger}\rangle\langle v_2^{associated}\rangle\cos(2\Delta\phi))$$

where v_2 is the second order harmonic in a Fourier expansion of the momentum anisotropy relative to the reaction plane, and must be subtracted in order to study the component associated with the jet. Systematic errors come from the errors on B, $\langle v_2^{trigger}\rangle$ and $\langle v_2^{associated}\rangle$. It is assumed that v_2 is the same for events with a trigger particle as for events without a trigger particle and that v_2 is roughly independent of $\Delta\eta$. For each data set $v_2(p_T)$ was fit in centrality bins to determine $\langle v_2^{trigger}\rangle$ and $\langle v_2^{associated}\rangle$. Details of the v_2 subtraction for Au + Au collisions at $\sqrt{s_{NN}} = 200$ GeV are given in [1] and for Cu + Cu collisions at $\sqrt{s_{NN}} = 200$ GeV in [9]. For Cu + Cu collisions at $\sqrt{s_{NN}} = 62.4$ GeV, the v_2 using the reaction plane as determined from tracks in the Forward Time Projection Chamber was used as the nominal value and the lower bound was determined from a multiplicity-dependent approximation as described for $\sqrt{s_{NN}} = 200$ GeV in [9]. For Au + Au collisions at $\sqrt{s_{NN}} = 62.4$ GeV, v_2 and its systematic errors were taken from [13]. B is fixed using the ZYAM method [14].

PYTHIA 8.1 was used to simulate $p + p$ collisions for comparisons to Y_{Jet}. A trigger particle was selected and the distribution of particles in azimuth was calculated, as in the experimental measurements. The yield was determined as the number of charged hadrons in the range $-1 < \Delta\phi < 1$. For comparisons to data identical limits on $p_T^{associated}$ and $p_T^{trigger}$ were applied. The minimum $\hat{p}_T$ is the parameter in PYTHIA for the transverse momentum in the hard subprocess [15]. A minimum value of $\hat{p}_T = 0.1$ GeV/c was used and 10^8 events were simulated to ensure that the minimum $\hat{p}_T$ did not affect the yield and that the statistical error was negligible. It was not necessary to study the distribution of particles in pseudorapidity since there is no *Ridge* in PYTHIA.

3 Results

3.1 The jet

Figure 1 compares the dependence of Y_{Jet} on $p_T^{trigger}$ for all systems and energies to the yield from PYTHIA 8.1 scaled by 2/3. An overall scaling factor of 2/3 was applied to the PYTHIA yields to match the data. The need for the scaling factor implies that PYTHIA assumes that too many particles are produced in hard processes, however, kinematic effects should still be reflected accurately in PYTHIA. The scaled PYTHIA yield describes the shape of the $p_T^{trigger}$ dependence well, with a few deviations at lower $p_T^{trigger}$. PYTHIA describes the energy dependence of Y_{Jet} well, indicating that the energy dependence can be explained as a pQCD effect. If Y_{Jet} is dominated by pQCD effects, deviations from PYTHIA at lower p_T would be expected. No system dependence is observed in the data, as would be expected for an effect dominated by pQCD.

The dependence of Y_{Jet} on $p_T^{associated}$ is shown in Fig. 2. As in Fig. 1, the scaled PYTHIA yield describes the shape of the data well and there is no system dependence. The inverse slope parameters from exponential fits to the data and to PYTHIA shown in Table 1 likewise support independence on collision system. Slight deviations from the scaled PYTHIA yield at lower $p_T^{associated}$ in Fig. 2 for collisions at $\sqrt{s_{NN}} = 62.4$ GeV are reflected in the inverse slope parameter, which is higher than that of the data.

Table 1 Inverse slope parameter k (MeV/c) of $p_T^{associated}$ for fits of data in Fig. 2. The inverse slope parameter from a fit to π^- as a function of p_T in Au + Au from [16] above 1.0 GeV/c is $k = 280.9 \pm 0.4$ MeV/c for $\sqrt{s_{NN}} = 62.4$ GeV and is $k = 330.9 \pm 0.3$ MeV/c for $\sqrt{s_{NN}} = 200$ GeV. Statistical errors only

	$\sqrt{s_{NN}} = 62.4$ GeV h-h	$\sqrt{s_{NN}} = 200$ GeV h-h
Au + Au Jet	317 ± 26	478 ± 8
Cu + Cu Jet	355 ± 21	445 ± 20
d + Au Jet		469 ± 8
PYTHIA	424 ± 5	473 ± 3

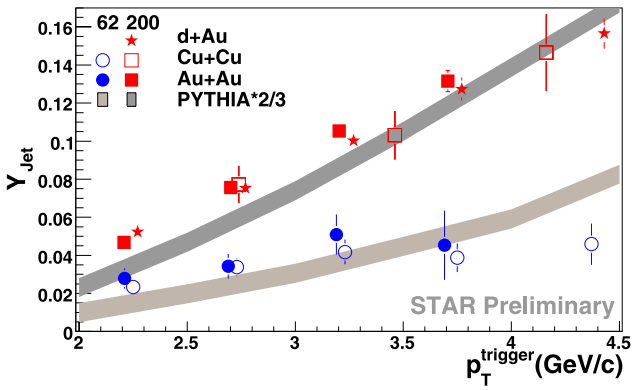

Fig. 1 (Color online) $p_T^{trigger}$ dependence of the Y_{Jet} for Cu + Cu and Au + Au at $\sqrt{s_{NN}} = 62.4$ GeV and d + Au, Cu + Cu, and Au + Au at $\sqrt{s_{NN}} = 200$ GeV compared to the yield from PYTHIA scaled by 2/3

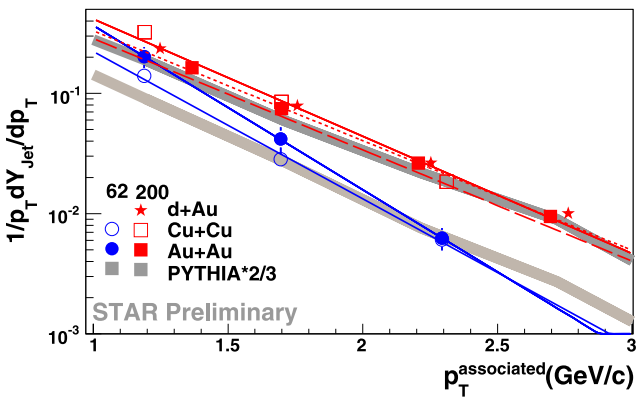

Fig. 2 (Color online) $p_T^{associated}$ dependence of Y_{Jet} for Cu + Cu and Au + Au at $\sqrt{s_{NN}} = 62.4$ GeV and d + Au, Cu + Cu, and Au + Au at $\sqrt{s_{NN}} = 200$ GeV compared to the yield from PYTHIA scaled by 2/3. The inverse slope parameters from fits of an exponential to the data and to PYTHIA are given in Table 1

The N_{part} dependence of Y_{Jet} is shown in Fig. 3 and compared to the scaled PYTHIA yield. In contrast to measurements at higher p_T, which show no N_{part} dependence, a small increase with N_{part} is observed. This may be caused by either slight modifications of the *Jet* which increase with system size or some of the *Ridge* being misidentified as part of the *Jet*. If the *Ridge* were not completely independent of $\Delta\eta$, some of the particles in the *Ridge* could be associated with the *Jet*. Since the *Ridge* has roughly four times as many particles than the *Jet* in central Au + Au, this would give a smaller relative error to the *Ridge* than the *Jet*. However, the *Jet* has also been observed to be considerably broader in $\Delta\eta$ in $A + A$ collisions than in $p + p$ and d + Au collisions [2, 10], which would imply modifications of the *Jet* in $A + A$ collisions. At this point models for *Jet* and *Ridge* production cannot distinguish these mechanisms.

That PYTHIA describes the $p_T^{trigger}$ and $p_T^{associated}$ dependence of Y_{Jet} fairly well implies that PYTHIA can be

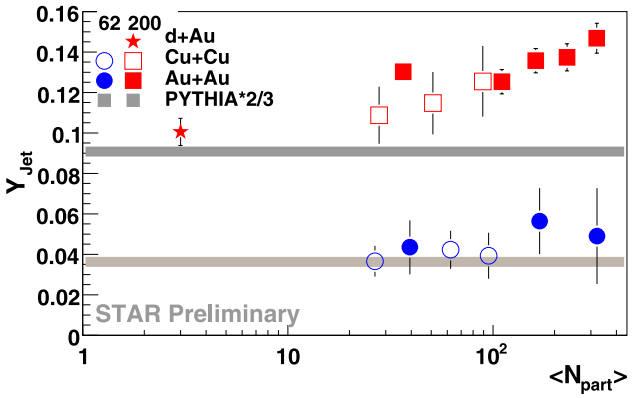

Fig. 3 (Color online) N_{part} dependence of the Y_{Jet} for Cu + Cu and Au + Au at $\sqrt{s_{NN}} = 62.4$ GeV and d + Au, Cu + Cu, and Au + Au at $\sqrt{s_{NN}} = 200$ GeV compared to the yield from PYTHIA

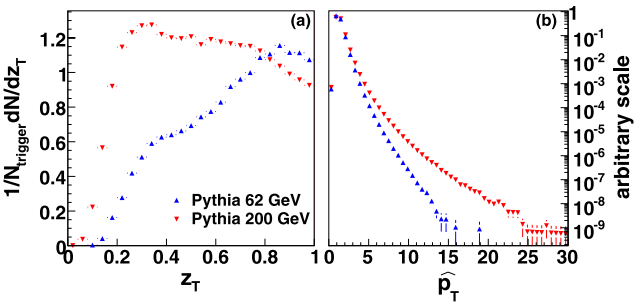

Fig. 4 (Color online) (**a**) distribution of trigger particles z_T and (**b**) $\hat{p}_T$ distribution in PYTHIA at $\sqrt{s_{NN}} = 62.4$ GeV from PYTHIA 8.1 for 1.5 GeV/c $< p_T^{associated} < p_T^{trigger}$ and 3.0 $< p_T^{trigger} <$ 6.0 GeV/c at $\sqrt{s_{NN}} = 62.4$ GeV and $\sqrt{s_{NN}} = 200$ GeV

used to approximate the momentum fraction carried by the leading hadron, z_T. Figure 4 shows the $\hat{p}_T$ distribution and the distribution of trigger particles in $z_T = p_T^{trigger}/\hat{p}_T$ predicted by PYTHIA for $\sqrt{s_{NN}} = 62.4$ GeV and $\sqrt{s_{NN}} = 200$ GeV. Figure 4(a) shows that for the same $p_T^{trigger}$ and $p_T^{associated}$, the mean z_T is higher in $\sqrt{s_{NN}} = 62.4$ GeV and therefore the mean jet energy is lower. Figure 4(b) shows that this is caused by the steeper spectrum at $\sqrt{s_{NN}} = 62.4$ GeV. The lower Y_{Jet} in collisions at $\sqrt{s_{NN}} = 62.4$ GeV results from the higher mean z_T and is dominantly a kinematic effect.

3.2 The ridge

The dependence of Y_{Ridge} on N_{part} is given in Fig. 5. In collisions at both $\sqrt{s_{NN}} = 62.4$ GeV and $\sqrt{s_{NN}} = 200$ GeV Y_{Ridge} increases with N_{part}. As seen in Fig. 3, the yield at $\sqrt{s_{NN}} = 62.4$ GeV is considerably smaller than at $\sqrt{s_{NN}} = 200$ GeV. Figure 6 shows the ratio Y_{Ridge}/Y_{Jet} and shows that this ratio does not depend on $\sqrt{s_{NN}}$. PYTHIA simulations demonstrated that the data at $\sqrt{s_{NN}} = 62.4$ GeV likely correspond to a lower jet energy, so this implies that Y_{Ridge} decreases with energy just like Y_{Jet}.

Few models have attempted to make quantitative predictions for Y_{Ridge}. An exception is the momentum kick model, which is consistent with data on the energy dependence of Y_{Ridge} [17]. The collision energy dependence of Y_{Ridge} is potentially a sensitive test of models because the dominant factor in collision energy dependence should be different for various classes of models. Models which involve parton energy loss due to interaction with the medium such as the momentum kick model should have a smaller *Ridge* at lower energy, as observed in the data, because the initial parton energy was lower. The radial flow+trigger bias model should predict a dependence of Y_{Ridge} on the amount of radial flow in the system. An analysis similar to [18] could yield predictions for the collision system and energy dependence. Plasma instability models [7] should depend on whether plasma instabilities are more or less likely in small systems and at lower energies. When more detailed calculations are available, it is likely that the data could exclude some production mechanisms.

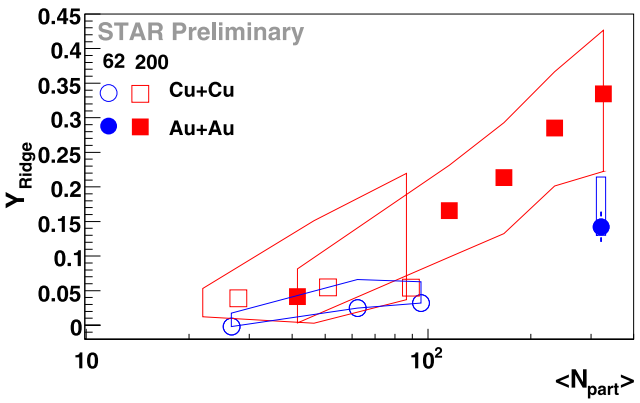

Fig. 5 (Color online) Y_{Ridge} dependence on N_{part} for $\sqrt{s_{NN}} = 62.4$ GeV and $\sqrt{s_{NN}} = 200$ GeV

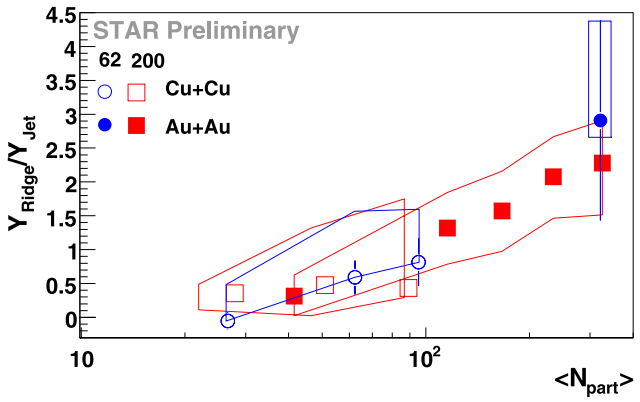

Fig. 6 (Color online) Y_{Ridge}/Y_{Jet} dependence on N_{part} for $\sqrt{s_{NN}} = 62.4$ GeV and $\sqrt{s_{NN}} = 200$ GeV

4 Conclusions

The data from $d + \mathrm{Au}$, $\mathrm{Cu} + \mathrm{Cu}$, and $\mathrm{Au} + \mathrm{Au}$ and $\sqrt{s_{NN}} = 62.4$ GeV and $\sqrt{s_{NN}} = 200$ GeV demonstrate that the *Jet* shows no system dependence. In addition, the collision energy dependence of Y_{Jet} is described well by PYTHIA even at fairly low p_T and the $p_T^{trigger}$ and $p_T^{associated}$ dependencies agree with PYTHIA up to a scaling factor, with a few deviations at lower p_T. This implies that the dominant production mechanism of the *Jet* is fragmentation. Deviations from PYTHIA may imply modifications of the *Jet* in $A + A$ collisions. It also implies that PYTHIA or other models can be used to determine the effect of the kinematic cuts on $p_T^{trigger}$ on the z_T and jet energy distribution, which could be very useful for the theoretical interpretation of the *Ridge*.

Y_{Ridge} is smaller at lower collision energies and increases with system size independent of collision system. There is no dependence on the collision system. Data on the collision energy and system dependence could provide a robust test of models, and comparisons of Y_{Jet} to PYTHIA imply that the effects of the kinematic cuts on the distribution of jet energies can be inferred from PYTHIA.

References

1. J. Bielcikova (STAR Collaboration), J. Phys. G **34**, S929–932 (2007)
2. J. Putschke (STAR Collaboration), J. Phys. G **34**, S679–683 (2007)
3. N. Armesto, C. Salgado, U. Wiedemann, Phys. Rev. C **72**, 064910 (2005)

4. C.Y. Wong, Phys. Rev. C **76**, 054908 (2007)
5. R. Hwa, C. Chiu, Phys. Rev. C **72**, 034903 (2005)
6. S. Voloshin, Phys. Rev. B **632**, 490 (2006)
7. A. Dumitru, Y. Nara, B. Schenke, M. Strickland, arXiv:0710.1223v2
8. K.H. Ackermann et al., Nucl. Inst. Methods A **499**, 624 (2003)
9. C. Nattrass (STAR Collaboration), J. Phys. G **35**, 044063 (2008)
10. M. Bombara (STAR Collaboration), J. Phys. G **35**, 044065 (2008)
11. B.B. Back et al., Phys. Rev. C **72**, 051901 (2005)
12. B.B. Back et al., Phys. Rev. Lett. **94**, 122303 (2005)
13. B.I. Abelev et al., Phys. Rev. C **75**, 054906 (2007)
14. J. Adams et al. (STAR Collaboration), Phys. Rev. Lett. **95**, 152301 (2005)
15. T. Sjöstrand et al., arXiv:0710.3820 [hep-ph]
16. B.I. Abelev et al. (STAR Collaboration), Phys. Lett. B **655**, 104 (2007)
17. C.Y. Wong, arXiv:0806.2154v1
18. C.A. Pruneau, S. Gavin, S.A. Voloshin, arXiv:0711.1991v2